Journal of Mining Institute. 2021. Vol. 247. p. 3-11
Dmitry I. Blokhin, Pavel N. Ivanov, Oleg L. Dudchenko
DOI: 10.31897/PMI.2021.1.1

UDC 539.4:539.5:539.8

Experimental study of thermomechanical effects in water-saturated limestones during their deformation

Dmitry I. BLOKHIN[1,2], **Pavel N. IVANOV**[2]✉, **Oleg L. DUDCHENKO**[2]
[1] *Institute of Comprehensive Exploitation of Mineral Resources Russian Academy of Sciences, Moscow, Russia*
[2] *National University of Science and Technology "MISiS", Moscow, Russia*

***How to cite this article*:** Blokhin D.I., Ivanov P.N., Dudchenko O.L. Experimental study of thermomechanical effects in water-saturated limestones during their deformation. Journal of Mining Institute. 2021. Vol. 247. p. 3-11. DOI: 10.31897/PMI.2021.1.1

Abstract. Stability control of elements of stone constructions of various structures is a prerequisite for their safe operation. The use of modern methods of non-destructive diagnostics of the stress-strain state of such constructions is an effective, and in many cases the only way to control it. Studies of thermal radiation accompanying the processes of solid bodies deformation allowed to justify and develop a method that allows to obtain non-contact information about changes in the stress-strain state in various types of geomaterials, including limestones. However, studies of the water saturation influence of rocks on the thermal radiation parameters recorded in this way are currently superficial. Taking into account the water saturation degree of rocks is necessary when monitoring the mechanical condition of stone structures that are in direct contact with water. The main purpose of this work is to study the dependences of changes in the intensity of thermal radiation from the surface of limestone samples with different humidity under conditions of uniaxial compression. The obtained results showed the expected significant decrease in the mechanical properties (uniaxial compressive strength and elastic modulus) of water-saturated samples in comparison with dry ones. At the same time, a significant increase in the intensity of thermal radiation of limestone samples subjected to compression with an increase in their water saturation was recorded, which makes it necessary to take into account the revealed regularity when identifying changes in the stress state of stone structures established according to non-contact IR diagnostics in real conditions.

***Key words*:** stone building constructions; limestone; water saturation; axial stresses; deformation; monitoring; IR radiation; laser-ultrasonic diagnostics

Acknowledgement. The work was supported by the Ministry of Science and Higher Education of the Russian Federation in the framework of the program for improving the competitiveness of the National University of Science and Technology "MISiS", adopted by Government Resolution N 211 of 16.03.2013 (grant N K2-2020-018).

Introduction. Natural stone, from which the most ancient structures are built, is now also effectively used in the construction of industrial and civil objects [3], for example, historical buildings, religious buildings, monuments, bridges, retaining walls, tunnels, and others. These engineering structures can be subjected to various dynamic loads of both natural and man-made nature (wind, earthquakes, vibrations, etc.) [3, 17]. Such loads negatively affect the stability of structures, being catalysts for destructive mechanical processes in the material. In this regard, the reliability assessment of the considered structures is an urgent task, for which it is necessary to use the procedures for monitoring the deformation processes in stone constructions.

Standard methods for measuring changes in the parameters of the stress-strain state (SSS) of building constructions involve the use of various modifications of deformometers that are placed either on the free surfaces of structures or in their body [1, 6, 9]. However, unlike concrete structures that have a relatively smooth surface, such placement of measuring sensors on the surface of stone structures can be difficult, and their location in the body of structural elements requires special work that violates their integrity, which may be unacceptable when analyzing historical or memorial structures. These circumstances determine the need for the use of non-destructive diagnostic methods in the investigation of stone constructions.

Currently, monitoring systems for the state of building constructions and rock masses use the methods that include measurements of variations in the parameters of physical fields of different nature that accompany the processes of deformation and destruction of materials [1, 9, 10, 17]. Among the actively developed methods of non-destructive diagnostics of the mechanical state of geomaterials is the method of IR radiometry, which uses the results of non-contact measurements of changes in the intensity of infrared radiation from the surface of rocks during their deformation [21, 15, 19, 22]. The interpretation of the thermoradiative IR measurements results is based on the description of the known thermodynamic effects: changes in the temperature of a solid body during its adiabatic deformation (thermoelastic and thermoplastic effects [2, 18]) and the dependence of the infrared radiation intensity from the body surface on the temperature [25].

In [21, 15, 19, 22], the effectiveness of IR radiometry for identifying the stages of deformation of various types of rocks was justified. However, in order to obtain reliable information about the course of deformation processes based on thermoradiation measurements in real conditions, it is necessary to study the variability influence of the physical and mechanical properties of rocks on the recorded thermal radiation parameters, in particular, taking into account the degree of water saturation of the studied materials when interpreting thermoradiation measurements, which has a significant impact on the physical and mechanical state of rocks [11, 20, 12, 27].

The purpose of this work is to study the phenomenon of these thermomechanical effects in structurally inhomogeneous rock samples with different humidity under uniaxial compression using non-contact IR measurements.

Methodology. Experiments were carried out on limestone samples – the most commonly used material of stone constructions [3, 20]. Since limestone belongs to rocks with a high degree of heterogeneity, a selection of samples with similar values of physical and mechanical parameters and similar structural properties was created in order to obtain high-quality and reasonable results when performing the described studies. For this purpose, a set of preliminary tests was carried out, including both standard methods for determining the physical and mechanical properties of rocks, and methods based on introscopic methods of investigation, such as scanning electron microscopy and laser ultrasonic diagnostics [4, 14, 24].

A solid block of limestone was cut into more than 100 parallelepipeds measuring 25 × 25 × 55 mm.

The mineral and elemental analyses were carried out on a series of 25 × 25 mm anslips using a Phenom ProX scanning electron microscope, which operates both in the optical image mode for petrographic analysis and in the electronic image mode, from which the elemental composition was determined on the basis of an energy-dispersion system. The analysis showed that for most samples the average content is, %: calcium 40.0-42.3, carbon 12.1-13.9, oxygen 45.1-47.5. A slight presence of various mineral components and impurities was found, %: silicon 0.2-0.3, magnesium 0.1-0.2, iron 0.1. The impurities were distributed evenly over the entire surface of the studied samples.

The surface of the studied anslips is represented by a granular structure. Pore systems occupying 5-7 % of the total surface area are recorded at the grain contact boundary; the values of characteristic pore sizes are in the range of 40-450 microns. The mineral composition is represented by calcite, the content of which varied in the range of 97.5-98.3, an insignificant amount of quartz-1.5-2.3 and dolomite-less than 0.5 %. The total contribution of the remaining minerals is small (less than 0.1 %).

Taking into account the electron microscopy data, 15 samples with similar structural properties were selected from the original series. At the second stage, it was necessary to select samples with approximately the same porosity values from this series. The porosity was evaluated using laser ultrasonic structurescopy [4, 14, 23], performed on an automated structuroscope UDL-2M on 15 plates with a size of 50 × 25 mm and a thickness of about 4-5 mm, made from selected samples.

DOI: 10.31897/PMI.2021.1.1

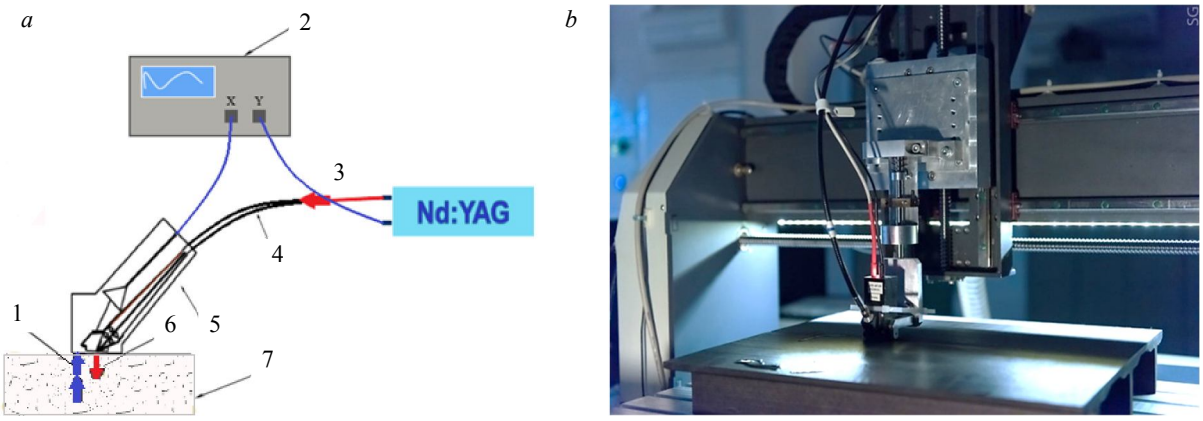

Fig. 1. Scheme (*a*) and appearance (*b*) of the laser-ultrasonic structuroscope UDL-2M
1 – reflected signals; 2 – analog-to-digital converter; 3 – short laser pulse; 4 – fiber-optic cable; 5 – laser-ultrasonic converter; 6 – probing acoustic pulses; 7 – test sample

The principle of the structurescope operation (Fig.1) is based on the registration of signals obtained as a result of the dispersal of broadband acoustic pulses on various inhomogeneities of samples [4].

Scanning was performed on the surface of the plate in 1 mm increments. Taking into account the thickness and time of the double path of the acoustic pulse along the sample, the distribution velocities V_l of the longitudinal waves were calculated at each scanning point. The velocity of the shear wave V_t was determined by the delay time of the shear wave relative to the reference signal. Local values of elastic wave velocities at 100 points of each sample were obtained. Table 1 shows the values of the average velocities of longitudinal and shear waves.

Table 1

Results of measurement of elastic wave velocities

Wave velocity, m/s	Sample number														
	1	2	3	4	5	6	7	8	9	10	11	12	13	14	15
V_l	4506	4185	4540	4520	4517	4758	4534	4501	4245	4526	4575	4289	4523	4534	4696
V_t	2409	2098	2420	2447	2408	2531	2403	2367	2006	2394	2454	2043	2336	2315	2574

According to the given data, it is possible to calculate the local porosity of the samples [13]:

$$P_{\text{total}} = \left(1 - \left(\frac{V_1}{V_0}\right)^2\right)^{\frac{3}{2}}, \quad (1)$$

where V_0 is the distribution velocity of the longitudinal wave in the material at $P_{\text{total}} = 0$, that is in the absence of porosity.

To calculate V_0, the following algorithm was developed. It is known that the main minerals contained in limestone (calcite and quartz) belong to the trigonal symmetry class [5]. In crystals of trigonal syngony only along three crystallographic axes [100], [010], [001] purely longitudinal waves propagate, the velocities V_1, V_2, V_3 of which are determined by the diagonal elements of the stiffness matrix C_{33}, C_{11} [5]:

$$\rho V_1^2 = C_{33}; \quad (2)$$

$$\rho V_2^2 = \rho V_3^2 = C_{11}, \quad (3)$$

where ρ is the crystal density.

DOI: 10.31897/PMI.2020.1.1

In all other directions, quasi-longitudinal waves spread, the phase velocities of which are determined from the Green – Christoffel equation [5], and their values can differ significantly from the values of the velocities of pure modes. Since calcite and quartz minerals in limestone are chaotically oriented, it is necessary to perform averaging in all directions to calculate the velocity V_{10}, which is a rather time-consuming procedure. Therefore, to estimate V_0 from the known values of the stiffness matrix coefficients $\{C_{ij}\}$, $i, j = 1, \ldots, 6$ for calcite and quartz, given in Table 2, the velocities V_1, V_2, V_3 were found along the crystallographic axes [100], [010], [001] and additionally in the directions [110], [011], [101] the velocities are V_{12}, V_{23}, V_{13} for each mineral [5]. Next, averaging was performed in all six directions, taking into account the contribution of calcite and quartz.

Table 2

Stiffness matrix coefficients for calcite and quartz

Rock	C_{11}, GPa	C_{12}, GPa	C_{44}, GPa	C_{33}, GPa	C_{13}, GPa	C_{66}, GPa	ρ, kg/m³
Calcite	137	45.2	34.2	79.2	44.8	45.9	2980
Quartz	86.8	7.1	58.3	105.9	–11.9	39.9	2650

As a result of the calculations, the average velocity V_0 in a limestone sample without pores was 4900 m/s. Figure 2 shows the results of the calculation of the porosity values of the samples, carried out according to the formula (1). Indicators of the total porosity P_{total} of the samples 1, 3, 4, 5, 7, 8, 10, 11, 13, 14 belong to a single interval, which is 13-14 %. These samples were subsequently subjected to mechanical tests.

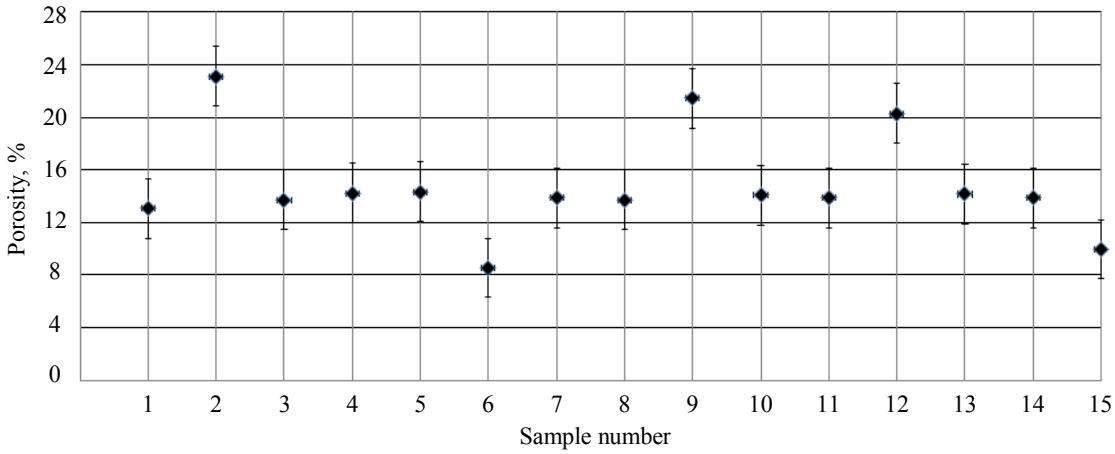

Fig.2. Porosity values for the studied limestone samples

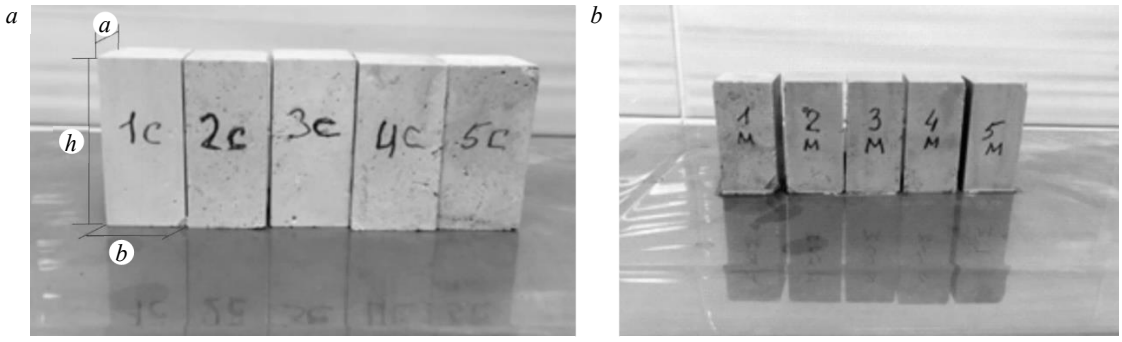

Fig.3. Dry (*a*) and water-saturated (*b*) limestone samples

Results. To conduct experiments to assess the effect of water saturation of limestone samples on the kinetics of thermal radiation accompanying their deformation, samples 1, 3, 4, 5, 7, 8, 10, 11, 13, 14 were selected and then divided into two groups (5 samples in each) (Fig.3). Samples of one group were placed in water for seven days. After that, the mass of the samples was determined and their density was calculated, the values of which are presented in Table 3.

Table 3

Geometric and density parameters of limestone samples

Sample number	m, g	a, mm	b, mm	$S = ab$, mm^2	h, mm	$V_{total} = Sh$	ρ, kg/m^3
Dry samples							
1c	67.18	25.65	23.50	603.28	50.29	30131	2216
2c	67.05	25.06	24.34	585.90	49.95	29215	2294
3c	66.98	25.15	24.10	581.02	50.07	29088	2312
4c	67.46	25.32	25.07	584.77	50.01	29212	2299
5c	67.05	25.50	25.50	650.25	50.27	32688	2251
Water-saturated samples							
1m	70.15	24.64	24.03	592.10	49.97	29587	2370
2m	69.26	24.42	24.36	594.87	50.28	29910	2315
3m	70.25	23.61	24.63	581.51	50.13	29151	2409
4m	70.09	24.50	24.56	601.72	50.54	30410	2304
5m	69.55	25.65	23.46	601.75	50.22	30219	2299

The average densities of dry and water-saturated samples were 2274 and 2340 kg/m^3, respectively.

The measurements were performed on the LFM-50 test machine using an automated system [22], which allows simultaneous recording of mechanical and thermoradiative parameters (Fig.4).

In the experiments, the RTN-31 detector was used as the primary receiver of IR radiation [21, 22], designed for non-contact measurement of changes in the intensity of optical radiation in the infrared frequency range. The IR radiation sensor 1 is installed approximately in the middle of the height of the sample 2 at a distance of 0.5-1 cm from the surface.

Graphs of changes in the time values of the output signals obtained as a result of the passage of the primary signal from the IR radiometer (RTN-31 detector) through the measuring and computing path during the deformation of dry $W_1(t)$ and water-saturated $W_2(t)$ limestone samples in the uniaxial compression mode at a constant loading rate ($d\sigma_1/dt = \text{const}$) are shown in Fig.5. The dependences $W_1(t)$ and $W_2(t)$ demonstrate the nature of changes in the intensity of IR radiation in time intervals corresponding to the intervals of the linear stage of limestone samples deformation.

The diagrams $\sigma_1 - \varepsilon_1$ obtained during the experiment are shown in Figure 6. The graphs $\sigma_1(\varepsilon_1)$ confirm the existence of a significant dependence of changes in the strength and deformation characteristics of limestone samples on the degree of their water saturation [22, 12]. In particular, the values of the ultimate strength for dry σ_{De} and water-saturated σ_{We} limestone samples determined from the graphs shown in Figure 6 differ by about 2.5 times ($\sigma_{De} \approx 74$ MPa and $\sigma_{We} \approx 30$ MPa).

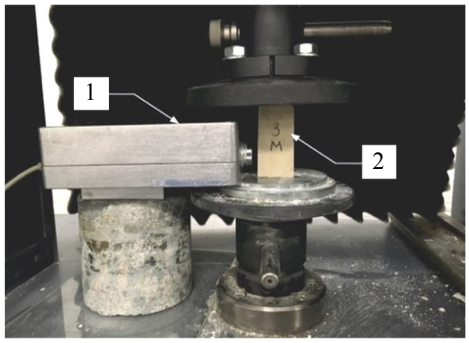

Fig.4. Experimental stand

DOI: 10.31897/PMI.2020.1.1

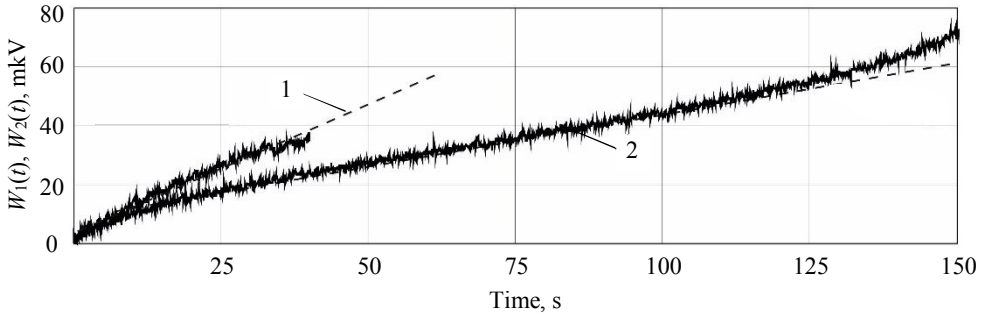

Fig.5. IR radiometry output signals for limestone samples
1 – dry; 2 – water-saturated

Discussion of the results. Analyzing the dependences $W_1(t)$ and $W_2(t)$, we can conclude that the angle of inclination of the straight line approximating the graph $W_2(t)$ is significantly greater than the angle of inclination of the corresponding straight line for the graph $W_1(t)$, which indicates a higher thermal activity of the water-saturated limestone sample. The obtained result is consistent with the conclusions of [8, 26], which also record an increase in the IR radiation intensity of rock samples subjected to compression with an increase in their water saturation. Changes in both the thermophysical and physico-mechanical characteristics of samples under the influence of water saturation are the main factor determining the observed thermomechanical effect.

During the analysis of the obtained results, to confirm their adequacy, it is possible to perform estimated calculations of temperature increments ΔT for dry and water-saturated samples. For this purpose, the well-known approximation [2, 18] is used, which relates the increments of the solid body stresses with temperature changes during its uniaxial adiabatic deformation,

$$\Delta T = \frac{\alpha}{\rho c} T_0 \Delta\sigma_1, \tag{4}$$

where T_0 – absolute value of the temperature before the start of deformation; α – linear expansion coefficient; c – specific heat capacity at constant pressure; ρ – material density.

Then, as follows from the expression (4), with the same increment of the solid body stresses $\Delta\sigma_1$ under its uniaxial adiabatic deformation, the relationship between the temperature changes ΔT for dry and water-saturated samples will take the following form [16]:

$$\frac{\rho_d c_d}{\alpha_d}\frac{\Delta T_d}{T_0} = \frac{\rho_w c_w}{\alpha_w}\frac{\Delta T_w}{T_0} \tag{5}$$

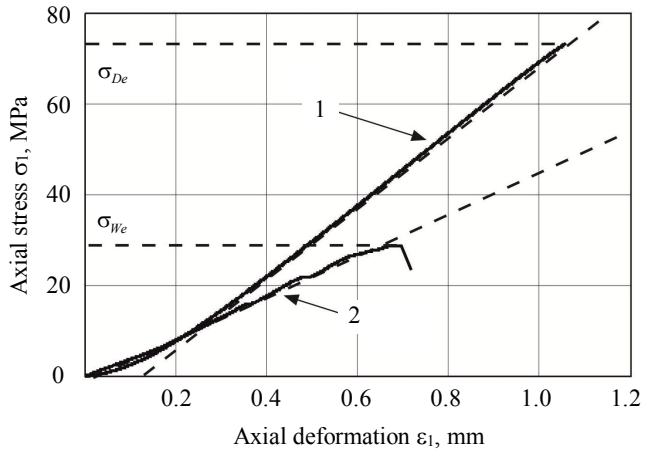

Fig.6. Dependence of stress on deformations σ_1-ε_1 for limestone samples
1 – dry; 2 – water-saturated

In [16], the validity of the relation is shown for different types of solid bodies

$$\alpha \sim \text{const} / \sqrt{E}, \tag{6}$$

where E is the elastic modulus of the material under uniaxial deformation.

The values of the E_d and E_w modules for dry and water-saturated samples, respectively, were calculated using the graphs $\sigma_1 - \varepsilon_1$ shown in Figure 6. Then the formula (5) will take the following form:

$$\rho_d c_d \sqrt{E_d}\Delta T_d = \rho_w c_w \sqrt{E_w}\Delta T_w. \tag{7}$$

The results of calculations of the elastic modulus values: $E_d = 69$ and $E_w = 42$ GPa.

For the calculations according to formula (7), the data from Table 3 were used.

In order to obtain approximate values of the specific heat capacity c for water-saturated and dry limestone samples, it is necessary to use the well-known definition [7], in which the specific heat capacity of a heterogeneous medium is understood as the arithmetic weighted average of all mineral components present in the medium with a fraction of k_i and their specific heat capacity c_i:

$$c = \sum c_i k_i. \tag{8}$$

Since the main material component of the test samples is calcite, the formula for calculating the specific heat capacity of water-saturated limestone was obtained from equation (8):

$$c_{\text{w}} = \sum c_i k_i = \frac{c_{\text{calc}} \rho_{\text{calc}} V_{\text{calc}} + c_{\text{water}} \rho_{\text{water}} V_{\text{water}} P_{\text{open}}}{\rho_{\text{m.w}} V_{\text{s}}}, \tag{9}$$

где c_{calc} – specific heat capacity of calcite; ρ_{calc} – calcite density; V_{calc} – calcite volume; c_{w} – specific heat capacity of water; ρ_{w} – water density; V_{w} – water volume; P_{open} – open porosity; $\rho_{\text{m.w}}$ – experimentally measured density of a water-saturated sample; V_{s} – sample volume.

The open porosity was determined by the Archimedes method in accordance with ASTM C830-00 (2016). The pore volume was determined by the difference in the mass of the dry and water-saturated sample, and the open porosity was determined by the formula

$$P_{\text{open}} = \frac{V_{\text{por.av}}}{V_{\text{av}}}. \tag{10}$$

According to the results of calculations, the average value of the open porosity was 9.5 %, while the total porosity P_{total} was 13.7 %. Considering that the calcite volume of is related to the total porosity P_{total}, including open P_{open} and closed ($P_{\text{total}} - P_{\text{open}}$), i.e. $V_{\text{calc}} = V_{\text{s}}(1 - P_{\text{open}})$, it is obtained

$$c_{\text{w}} = \sum c_i k_i = \frac{c_{\text{calc}} \rho_{\text{calc}} (1 - P_{\text{total}}) + c_{\text{water}} \rho_{\text{water}} P_{\text{open}}}{\rho_{\text{m.w}}}. \tag{11}$$

Similarly, an expression is obtained for calculating the specific heat capacity of dry limestone:

$$c_{\text{d}} = \sum c_i k_i = \frac{c_{\text{calc}} \rho_{\text{calc}} (1 - P_{\text{total}})}{\rho_{\text{m.d}}}. \tag{12}$$

The heat capacity of the air, which is concentrated in the pores of the dry sample, is not taken into account. The results of calculating the specific heat capacities for dry c_{d} and water-saturated c_{w} samples according to formulas (11) and (12) are presented in Table 4.

Table 4

Results of calculation of specific heat capacity for samples

Dry samples		Water-saturated samples	
Sample number	c, J/(kg*K)	Sample number	c, J/(kg*K)
1c	1059	1m	1149
2c	1023	2m	1177
3c	1015	3m	1131
4c	1021	4m	1182
5c	1044	5m	1185
Average value	1032	Average value	1165

Further calculations using formula (6) involve the average values of specific heat capacities for dry and water-saturated samples, shown in Table 4. In addition, in the calculations, $T_0 = 300$ K.

Substituting in formula (7) the values necessary for the calculation, we obtain that the temperature increment for water-saturated samples is $\Delta T_w \approx 1.2\Delta T_d$, which is confirmed by the experimental dependences shown in Figure 5.

Thus, the conducted complex experimental studies, supported by the performed estimated calculations, demonstrate a significant influence of the water saturation of porous materials on their mechanical and thermophysical characteristics, which are expressed in a significant thermal activity increase initiated by the deformation processes occurring in them.

Conclusion. The conducted studies demonstrate a comprehensive approach to the laboratory study of thermomechanical processes in complexly structured heterogeneous materials subjected to deformation, which are limestone samples.

Using standard methods of scanning electron microscopy, a petrographic analysis was carried out and the structural features of the studied samples were revealed. The efficiency of using the data of laser-ultrasonic structroscopy for quantitative rapid assessment of the porosity of rocks is shown.

The dependences of changes in the intensity of thermal radiation $W(t)$ from the surface of limestone samples with different humidity under uniaxial compression conditions are obtained. An important element of the conducted experiments was the synchronous registration of variations in the intensity of thermal radiation and changes in mechanical parameters. Analysis of the data of combined measurements of axial stresses and deformations showed an expected significant decrease in the mechanical properties (uniaxial compressive strength and elastic modulus) of water-saturated samples compared to dry ones. The results of IR-radiometric measurements showed a clear dependence of the $W(t)$ graphs nature on the degree of water saturation of the test samples, which makes it necessary to take into account the revealed regularity when identifying changes in the stress state of the stone constructions elements in real conditions.

The authors are grateful to Professor V.I.Sheinin (Gersevanov Research Institute of Bases and Underground Structures (*NIIOSP*) *for his attention to the work and Professor E.B.Cherepetskaya* (*National University of Science and Technology "MISiS"*) *for their assistance in conducting laser-ultrasound studies.*

REFERENCES

1. Basov A.D., Romanevich K.V. Experimental Study of the Rocks and Lining Stress-Strain State During Construction of a Tunnel the Sochi-Adler Section of the North Caucasian Railroad. *Engineering Geology*. 2013. N 6, p. 28-37 (in Russian).

2. Gilyarov V.L., Slutsker A.I. Description of the thermoelastic effect in solid bodies in a wide temperature range. *Fizika tverdogo tela*. 2014. Vol. 56. Iss. 12, p. 2407-2409 (in Russian).

3. Ulyakov M.S., Sorokin I.S., Maganeva A.V., Ishtakbaev R.F. The use of natural stone by man: the path from antiquity to modern architecture. Dobycha, obrabotka i primenenie prirodnogo kamnya: Sbornik nauchnykh trudov. Vol. 14. Magnitogorsk: MGTU im. G.I.Nosova, 2014, p. 263 (in Russian).

4. Vinnikov V.A., Cherepetskaya E.B., Zakharov V.N., Malinnikova O.N. Investigation of the structure and elastic properties of geomaterials using contact broadband ultrasonic structurescopy. *Gornyi zhurnal*. 2017. N 4, p. 29-32. DOI: 10.17580/gzh.2017.04.05 (in Russian)

5. Kapitonov A.M., Vasilev V.G. Physical properties of rocks in the western part of the Siberian Platform. Moscow: Infra-m, 2018, p. 424 (in Russian).

6. Oparin V.N., Annin B.D., Chugui Yu.V. et al. Methods and measuring devices for modeling and field studies of nonlinear deformation-wave processes in block rock masses. Novosibirsk: Izdatelstvo Sibirskogo otdeleniya Rossiiskoi akademii nauk, 2007, p.330 (in Russian).

7. Lyukshin P.A., Lyukshin B.A., Matolygina N.Yu., Panin S.V. Determination of the effective thermophysical characteristics of the composite material. *Fizicheskaya mezomekhanika*. 2008. Vol. 11. N 5, p. 103-110 (in Russian).

8. An Experimental Study on Infrared Radiation Characteristics of Sandstone Samples Under Uniaxial Loading / L.Ma, Y.Zhang, K.Cao, Z.Wang. *Rock Mechanics and Rock Engineering*. 2019. Vol. 52. P. 3493-3500. DOI: 10.1007/s00603-018-1688-6

9. Wu Y., Li S., Wang D., Zhao G. Damage monitoring of masonry structure under in-situ uniaxial compression test using acoustic emission parameters. *Construction and Building Materials*. 2019. Vol. 215, p. 812-822. DOI: 10.1016/j.conbuildmat.2019.04.192

10. Carpinteri A., Iacidogna G., Borla O., Manuello A., Niccolini G. Electromagnetic and neutron emissions from brittle rocks failure: experimental evidence and geological implications. *Sadhana*. 2012. Vol. 37. N 1, p. 59-78. DOI:10.1007/s12046-012-0066-4

11. Si W., Di B., Wei J., Li Q. Experimental study of water saturation effect on acoustic velocity of sandstones. *Journal of Natural Gas Science and Engineering*. 2016. Vol. 33, p. 37-43. DOI: 10.1016/j.jngse.2016.05.002

12. Lu Y., Wang L., Sun X., Wang J. Experimental study of the influence of water and temperature on the mechanical behavior of mudstone and sandstone. *Bulletin of Engineering Geology and the Environment*. 2017. Vol. 76, p. 645-660. DOI: 10.1007/s10064-016-0851-0

13. Karabutov A.A., Podymova N.B., Cherepetskaya E.B. Measuring the dependence of the local Young's modulus on the porosity of isotropic composite materials by a pulsed acoustic method using a laser source of ultrasound. *Journal of Applied Mechanics and Technical Physics*. 2013. Vol. 54, p. 500-507. DOI: 10.1134/S0021894413030218

14. Karabutov A.A., Podymova N.B., Cherepetskaya E.B. Determination of uniaxial stresses in steel structures by the laser-ultrasonic method. *Journal of Applied Mechanics and Technical Physics*. 2017. Vol. 58, p. 503-510. DOI: 10.1134/S0021894417030154

15. Lou Q., He X. Experimental study on infrared radiation temperature field of concrete uniaxial compression. *Infrared Physics & Technology*. 2018. Vol. 90, p. 20-30. DOI: 10.1016/j.infrared.2018.01.033

16. Zhao S., Zhang G., Sun R., Wong C. Multifunctionalization of novolac epoxy resin and its influence on dielectric, thermal properties, viscoelastic, and aging behavior. *Journal of Applied Polymer Science*. 2014. Vol. 131. Iss. 8. DOI: 10.1002/app.40157

17. Ohtsu M. Overview of visualized NDE for on-site measurement. Innovative AE and NDT Techniques for On-Site Measurement of Concrete and Masanry Structures: State-of-the-Art Reports of the RILEM Technical Commitee 239-MCM. Springer, 2016, p. 173-176. DOI: 10.1007/978-94-017-7606-6_10

18. Plekhov O.A. Experimental study of thermodynamics of plastic deformation by infrared thermography. *Technical Physics. The Russian Journal of Applied Physics*. 2011. Vol. 56. N 2, p. 301-304. DOI: 10.1134/S106378421102023X

19. Wu L., Liu S., Wu Y., Wang C. Precursors for Fracturing and Failure. Part II: IRR T – Curve Abnormalities. *International Journal of Rock Mechanics and Mining Sciences*. 2006. Vol. 43. Iss. 3, p. 483-493. DOI: 10.1016/j.ijrmms.2005.09.001

20. Rabat Á., Cano M., Tomás R. Effect of water saturation on strength and deformability of building calcarenite stones: Correlations with their physical properties. *Construction and Building Materials*. 2020. Vol. 232. 117259. DOI: 10.1016/j.conbuildmat.2019.117259

21. Sheinin V.I., Blokhin D.I. Features of thermomechanical effects in rock salt samples under uniaxial compression. *Journal of Mining Science*. 2012. Vol. 48. Iss. 1, p. 39-45. DOI: 10.1134/S1062739148010054

22. Sheinin V.I., Blokhin D.I., Novikov E.A., Mudretsova L.V. Study of Limestone Deformation Stages on The Basis of Acoustic Emission and Thermomechanical Effects. *Soil Mechanics and Foundation Engineering*. 2020. Vol. 56. N 6, p. 398-401. DOI: 10.1007/s11204-020-09621-y

23. Bychkov A., Simonova V., Zarubin V. et al. The progress in photoacoustic and laser ultrasonic tomographic imaging for biomedicine and industry: A review. *Applied Sciences* (Switzerland). 2018. Vol. 8 (10). DOI: 10.3390/app8101931

24. Victorov S.D., A Kochanov.N., Pachezhertsev A.A. Experimental study of the microstructural characteristics of the surfaces and volumes of granite samples. *Bulletin of the Russian Academy of Sciences: Physics*. 2018. Vol. 82. N 7, p. 786-788.

25. Vavilov V.P., Burleigh D.D. Review of pulsed thermal NDT: Physical principles, theory and data processing. *NDT and E International*. 2015. Vol. 73, p. 28-52. DOI: 10.1016/j.ndteint.2015.03.003

26. Cai X., Zhou Z., Tan L. et al. Water Saturation Effects on Thermal Infrared Radiation Features of Rock Materials During Deformation and Fracturing. *Rock Mechanics and Rock Engineering*. 2020, p. 1-18. DOI: 10.1007/s00603-020-02185-1

27. Shi X., Cai W., Meng Y. et al.Weakening laws of rock uniaxial compressive strength with consideration of water content and rock porosity. *Arabian Journal of Geosciences*. 2016. Vol. 9. N 5, p. 1-7. DOI: 10.1007/s12517-016-2426-6

Authors: **Dmitry I. Blokhin,** *Candidate of Engineering Sciences*, *Associate Professor*, *dblokhin@yandex.ru, https://orcid.org/0000-0002-4652-661X* (*Institute of Comprehensive Exploitation of Mineral Resources Russian Academy of Sciences, Moscow, Russia, National University of Science and Technology "MISiS", Moscow, Russia*), **Pavel N. Ivanov,** *Postgraduate Student, pavelnivanov@mail.ru, https://orcid.org/0000-0001-6958-5164* (*National University of Science and Technology "MISiS", Moscow, Russia*), **Oleg L. Dudchenko,** *Candidate of Engineering Sciences*, *Associate Professor*, *dionis_4444@mail.ru, https://orcid.org/0000-0002-9040-4433* (*National University of Science and Technology "MISiS", Moscow, Russia*).

The authors declare no conflict of interests.

The paper was received on 30 July, 2020.
The paper was accepted for publication on 2 March, 2021.